Bioresource Technology Reports 34 (2026) 102754

Contents lists available at ScienceDirect

Bioresource Technology Reports

journal homepage: www.sciencedirect.com/journal/bioresource-technology-reports

Sequential cascade biorefinery for the valorization of spent coffee grounds: Energy, biodiesel, furfural, and biochar production

Javier Mauricio Loaiza [a,*], Alberto Palma [a], Juan Carlos Garcia [a], Manuel Jesús Diaz [a], Ascensión Alfaro [b]

[a] Research Centre for Technology of Products and Chemical Processes (PRO2TECS), Department of Chemical Engineering, University of Huelva, Av. 3 de Marzo S/N, 21071, Huelva, Spain

[b] Agroforestry Department, University of Huelva, 21071, Huelva, Spain

ARTICLE INFO

Keywords:
Coffee grounds
Circular economy
Biorefinery
Biodiesel
Hemicelluloses

ABSTRACT

This study presents a sequential biorefinery approach for the integrated valorization of spent coffee grounds (SCG) within a circular economy framework. The process comprises multiple operational units. Initially, SCG are pelletized for direct combustion, demonstrating promising energy potential. In the second unit, coffee oil is extracted via Soxhlet using hexane, isopropanol, and ethanol, and subsequently converted into biodiesel through transesterification, yielding a biofuel with a favorable fatty acid profile. The third unit involves ultrasound-assisted cold alkaline extraction (CAE) of the residual solid to selectively recover hemicelluloses with minimal degradation. Optimal CAE conditions (40 °C, 90 min, 100 g L^{-1} NaOH) enhanced hemicellulose yield while maintaining high calorific value (21.529 kJ kg^{-1}), comparable to the raw material (21.560 kJ kg^{-1}). The hemicellulose-rich liquor was subjected to acid hydrolysis for furfural production, with maximum yield (590.3 mg L^{-1}) achieved under central experimental conditions (2% acid, 160 °C). The solid residue from hydrolysis underwent pyrolysis to produce biochar. Kinetic analysis of the pyrolysis process using the Flynn–Wall–Ozawa method on TGA data enabled determination of activation energy without assuming a specific reaction model. The results confirm the feasibility of integrating thermochemical and biochemical pathways for SCG valorization, supporting the development of sustainable biorefineries and contributing to renewable energy and chemical production within circular economy strategies.

1. Introduction

Coffee is one of the most consumed beverages worldwide and ranks as the second most traded commodity after petroleum (Kovalcik et al., 2018). Its large-scale consumption generates significant amounts of spent coffee grounds (SCG), estimated at around 6.5 million tons annually (Forcina et al., 2023; Jeníček et al., 2022). SCG is mainly produced during roasting and instant coffee manufacturing, representing 40–45% of fresh coffee cherries (Atabani and Al-Rubaye, 2022). Due to its abundance, low cost, and non-seasonal availability, SCG is considered an attractive feedstock for industrial applications without competing with food production (Al-Hamamre et al., 2012).

Despite its potential, most SCG is still disposed of as waste, posing environmental challenges and representing an underutilized resource. This study proposes a cascade biorefinery approach for SCG valorization through sequential processes to obtain energy, biodiesel, furfural, and biochar, aiming to maximise resource efficiency and sustainability.

Recent research has focused on the valorization of coffee residues through biorefineries, mainly by recovering individual fractions such as oils, bioenergy, nutrients, and compounds for food or environmental applications, with growing attention to spent coffee grounds (SCG) (Anagnostopoulou et al., 2024; Lauberts et al., 2022; Massaya et al., 2019; Mata et al., 2018). However, integrated cascading processes remain scarcely explored, which limits progress toward a circular bioeconomy and sustainable coffee industry.

SCG is a heterogeneous matrix rich in cellulose, hemicellulose, and lignin, and also contains high-value compounds such as fatty acids, phenolic antioxidants, and caffeine (Araujo et al., 2022; Battista et al., 2020b; Ramalakshmi et al., 2009). Despite this potential for multiple applications in bioenergy, cosmetics, and food, most SCG is still

* Corresponding author.
E-mail addresses: javiermauricio.loaiza@diq.uhu.es (J.M. Loaiza), alberto.palma@diq.uhu.es (A. Palma), juan.garcia@diq.uhu.es (J.C. Garcia), dblanco@diq.uhu.es (M.J. Diaz), ascension.alfaro@dcaf.uhu.es (A. Alfaro).

https://doi.org/10.1016/j.biteb.2026.102754
Received 18 February 2026; Received in revised form 23 March 2026; Accepted 10 April 2026
Available online 13 April 2026
2589-014X/© 2026 The Author(s). Published by Elsevier Ltd. This is an open access article under the CC BY license (http://creativecommons.org/licenses/by/4.0/).

incinerated or landfilled, representing an underutilized resource.

In addition to its use as a feedstock for biofuels, SCG can also serve as a direct source of renewable energy after drying or in the form of briquettes, thanks to its high calorific value (above 21.5 MJ kg^{-1}) (Colantoni et al., 2021; Kansai et al., 2018). From a life cycle perspective, using coffee briquettes could reduce air emissions by 76% compared to landfill disposal, while composting and biodiesel production offer improvements of 18% and 1%, respectively (Forcina et al., 2023).

SCG contains a considerable amount of lipids (fatty acids), specifically 10–15% by weight (Couto et al., 2009; Obruca et al., 2015), which can be extracted and transformed into biodiesel through their transesterification into fatty acid methyl esters (FAME) (Al-Hamamre et al., 2012). Coffee produces more oil per surface unit than other traditional crops, with an estimated production of 386 kg ha^{-1} compared to 375 kg ha^{-1} of soy production (Atabani and Al-Rubaye, 2022). Coffee oils present several advantages, such as being a source of non-edible oils, thus constituting an alternative to the limited availability of vegetable oil (Phan and Phan, 2008); moreover, they present high contents of antioxidants, which make them stable and hinder their decomposition (Al-Hamamre et al., 2012). On the other hand, most of the carbohydrates of SCG are hexoses, which facilitates the production of bioethanol, since they can be easily released in a single step by previously using soft treatments such as dilute acid hydrolysis (Araujo et al., 2022).

In the present work, the initial fractionation stages focused on oil recovery, as SCG is considered a promising substrate for biodiesel production due to its high oil content, which ranges between 10% and 24% by weight (Al-Hamamre et al., 2012; de Melo et al., 2014; Somnuk et al., 2017). These values are comparable to those of conventional raw materials such as sugarcane (13–20%) and corn (4–8%), although corn oil is mainly obtained from germ coproducts, which contain 25–50% oil (Arora and Singh, 2020; Barrera-Arellano et al., 2019). Literature reports SCG oil extraction yields between 11.8% and 15.3% (Al-Hamamre et al., 2012; de Melo et al., 2014), using techniques such as Soxhlet extraction with solvents like hexane, ethanol, methanol, and others (Acevedo et al., 2013; Efthymiopoulos et al., 2018; Ribeiro et al., 2024), and supercritical fluid extraction (SFE) (Ahangari and Sargolzaei, 2013; Coelho et al., 2020; Couto et al., 2009; Kanaan et al., 2025).

Hexane remains one of the most widely used solvents, applied through different operational methodologies, including accelerated solvent extraction, reflux, batch reactors, and pilot-scale systems (Al-Hamamre et al., 2012; Efthymiopoulos et al., 2019; Kondamudi et al., 2008; Sarno and Iuliano, 2018). For SFE, carbon dioxide is the most employed supercritical fluid due to its high purity, non-toxicity, low cost, and relatively mild critical conditions (31.1 °C and 72.8 bar), although ethanol is often used as a co-solvent to enhance solvation power (Couto et al., 2009; Ribeiro et al., 2024). While SFE minimizes solvent use, its high equipment cost limits accessibility compared to ethanol-based processes, which are more economical, allow solvent reuse, and operate under milder conditions, reducing degradation of sensitive compounds and improving sustainability (de Melo et al., 2014; Ribeiro et al., 2024).

In this work, cold alkaline extraction (CAE) was applied after oil removal to recover hemicelluloses from SCG, as these polysaccharides are key bioresources for producing alternative biofuels and biochemicals (Khemthong et al., 2021). CAE was chosen over other alkaline or hydrolysis treatments due to its operational and environmental advantages (García et al., 2013; Jiménez et al., 1999; Lozano-Calvo et al., 2024; Negawo et al., 2017). This technique enables selective hemicellulose extraction with minimal degradation and simple separation by alcoholic precipitation (Cheng et al., 2011; García et al., 2013; Steinbach et al., 2017). Performed at mild temperatures (20–40 °C) and without high pressures, CAE reduces energy consumption and uses non-corrosive, environmentally friendly chemicals (Carvalho et al., 2016; Kim et al., 2016). Additionally, the recovered hemicelluloses can be used as food additives or in the production of furfural and polymers (Pereira et al., 2019).

The process can be enhanced by ultrasound assistance, which reduces solvent use and extraction time while increasing hemicellulose yield (Ahangari and Sargolzaei, 2013; Goh et al., 2020; Lozano-Calvo et al., 2024). Ultrasound promotes acoustic cavitation, generating microbubbles that collapse and release localized shock waves and heat, disrupting the crystalline structure of solids (Ashokkumar, 2011). This clean and ecological method improves fractionation efficiency and selectivity, producing liquids richer in hemicelluloses and lignin compared to conventional processes (Ali and Saikia, 1997; García et al., 2011; Lozano-Calvo et al., 2024).

Furfural, a target compound in this work, is an important organic chemical obtained exclusively from lignocellulosic biomass, as no synthetic route exists for its industrial production (Lichtenthaler and Peters, 2004; Lozano-Calvo et al., 2024). It is produced through the acid-catalyzed dehydration of pentoses—mainly xylan and arabinan—present in hemicelluloses. This reaction can occur with or without added mineral acids, since acetyl groups in hemicelluloses release acetic acid during hydrolysis. Industrial processes require biomass with at least 15–20% pentose content, although only about one-third of this fraction is converted into furfural (Colantoni et al., 2021).

Furfural is highly valued for its thermosetting properties, mechanical strength, and corrosion resistance (Zeitsch, 2000). It serves as a selective solvent in lubricant production and as a precursor for plastics and phenolic resins (Araujo et al., 2022). Additionally, it is used to synthesize key non-petroleum chemicals such as furan, tetrahydrofuran, and furfurylic acid, and finds applications as a fungicide and nematocide in food, pharmaceutical, and agricultural industries (García et al., 2019; López et al., 2014; Yemis and Mazza, 2012).

One of the final processes in the treatment chain is pyrolysis, an innovative thermochemical method for converting residues into value-added products (Bartolucci et al., 2024; Wang et al., 2020). It involves the thermal decomposition of biomass in the absence of oxygen at temperatures between 300 and 700 °C (Amenaghawon et al., 2021), producing mainly bio-oil, biochar, and non-condensable gases such as H_2, CO, CO_2, and CH_4 (Gogoi et al., 2023). Compared to combustion and gasification, pyrolysis operates at lower temperatures, generates fewer pollutants, and improves ash quality, making it an effective strategy for bioenergy production and greenhouse gas mitigation (Vuppaladadiyam et al., 2023).

Pyrolysis technologies are classified as slow, fast, and flash pyrolysis (Mohan et al., 2006). Flash pyrolysis, characterised by high heating rates and short vapor residence times, favours bio-oil production (Bridgwater, 2012), whereas slow pyrolysis, with lower heating rates and longer residence times, yields more biochar through progressive carbonization (Kan et al., 2016). Bio-oil consists of an organic phase rich in hydrocarbons and a water-based phase containing esters, aldehydes, ketones, phenols, and acids (Butler et al., 2011; Dhyani and Bhaskar, 2018). To improve its quality for fuel applications, bio-oil requires catalytic or non-catalytic treatments to remove oxygen, nitrogen, and sulfur compounds, which otherwise reduce calorific value and increase pollutant emissions (Mettler et al., 2012; Zhang et al., 2005).

The gaseous fraction, mainly H_2 and CO at high temperatures, can be used in Fischer–Tropsch synthesis to produce liquid hydrocarbons, while its analysis is essential to assess environmental impact and energy potential (Vuppaladadiyam et al., 2023). Thermogravimetric analysis (TGA) provides valuable insights into pyrolysis kinetics by measuring weight loss as a function of temperature and time (Wang et al., 2020).

This study demonstrates the comprehensive valorization of spent coffee grounds (SCG) through a cascade biorefinery approach, integrating sequential processes to obtain biodiesel, hemicelluloses, furfural, biochar, and renewable energy. By exploiting the full potential of SCG, this strategy not only reduces waste and environmental impact but also generates high-value products that can replace petroleum-based alternatives. The proposed scheme contributes to advancing circular bioeconomy principles in the coffee sector, offering a sustainable

pathway for industrial residues and reinforcing the role of biorefineries in achieving resource efficiency and climate goals.

2. Materials and methods

2.1. General scheme of work

2.2. Characterisation and storage of raw materials

SCG was collected from the cafeterias of "El Carmen" campus of the University of Huelva (Spain), with an estimated generation of 50 kg of this residue per week, approximately. Once the SCG was received, the samples were prepared and moisture was extracted in a drying stove at 60 °C until reaching 3–6% of water. Moisture was determined by constant weight drying at 105 °C, in compliance with TAPPI T264-cm-07 (TAPPI T264-cm-07, 2007).

After preparing the raw material, its chemical composition was characterised. Firstly, we measured the extractable compounds that determine the amount of non-volatile soluble matter in neutral organic solvents, in compliance with TAPPI T204 cm-07, 2007 (TAPPI T204 cm-07, 2007).

Next, a quantitative acid hydrolysis (QAH) was performed in two stages. In the first stage, which was carried out with H_2SO_4 at 72%, the polysaccharides are broken down into oligomers. In the second stage, with H_2SO_4 at 4%, the oligomers are broken down into monomers. By determining the concentration of the monomers, it is possible to calculate the content of polysaccharides of the initial sample. The residue that remains after completing the QAH is the so-called Klason lignin.

The liquid obtained from the QAH was analysed in accordance with TAPPI T249 cm-09, 2009 (TAPPI T249 cm-09, 2009), for the determination of monomeric sugars (glucose, xylose, arabinose), and acetic acid, through high-performance liquid chromatography (HPLC), (Bio-Rad Laboratories, USA) with an Aminex HPX-87H ion-exchange column at 30 °C as stationary phase and 0.005 M H_2SO_4 at a flow-rate of 0.6 mL min^{-1} as mobile pase.

2.3. Determination of the gross heating values

The gross heating values (constant volume) were determined according to (CEN/TS14918, 2005) and (UNE 16001 EX., 2005), using a Parr 6300 automatic isoperibol (bomb) calorimeter (Parr Instrument Company, Moline, IL, USA), a CGA 540 connector, 99.5% pure oxygen, and a maximum pressure of 2500 psig and 1.0 g of pellets in each run.

Furthermore, the solid was subjected to elemental analysis (C, N, O, and H) using a C/H/S-Analyzer autosampler Eltra Helos.

2.4. Extraction and characterisation of coffee oil, transesterification process, and determination of the fatty acid profile

After the preliminary evaporation of the moist content, the SCG was subjected to solid-liquid extraction of coffee oils. The operation was previously optimised for the extraction of long-chain fatty acids (LCFAs), which represent the main substrates involved in the transesterification process for the production of biodiesel. Particularly, n-hexane, isopropanol and ethanol were employed for the extraction of coffee oils in a Soxhlet extractor, in accordance with TAPPI T204 cm-07 (TAPPI T204 cm-07, 2007).

To conduct the transesterification, the analysis consisted in the evaporation of the extract obtained by Soxhlet in a rotary evaporator at 55 °C. Subsequently, 8 mL of methanol (MeOH) and a pellet of

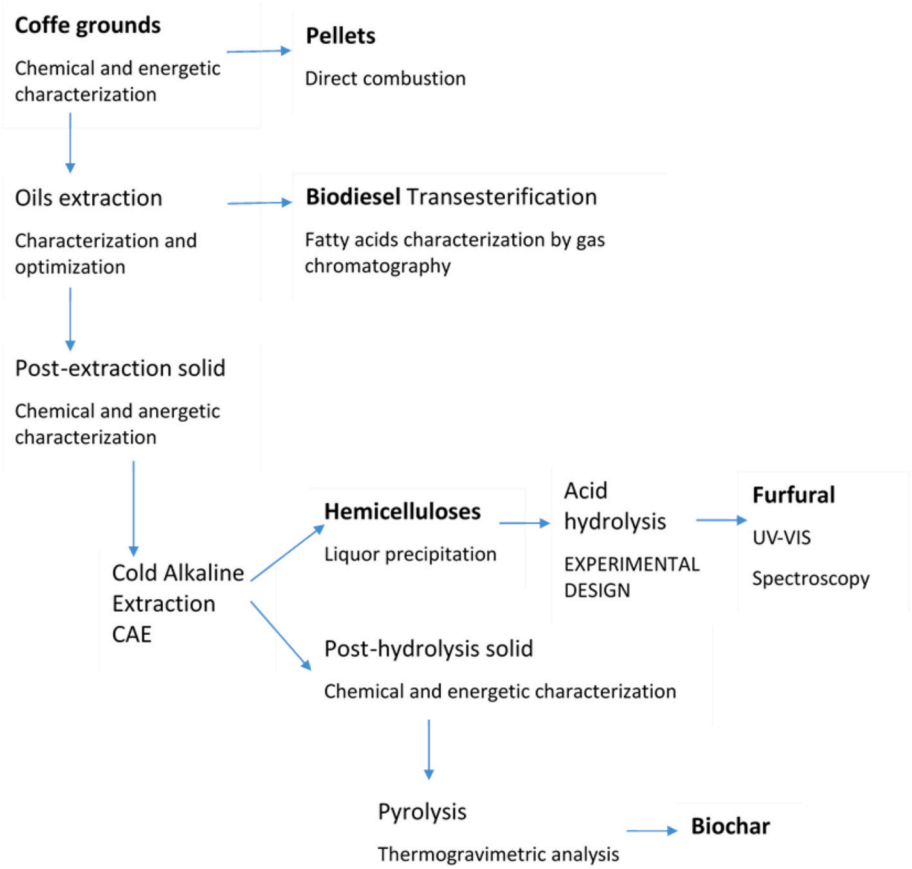

Fig. 1. Show a general scheme of experimental work carried out.

potassium hydroxide (KOH) of approximately 0.140 g were added to 1 mL of the extract, heating the mixture at 60 °C for 2 h. The reaction was terminated through KOH neutralisation with acetic acid (CH_2COOH) in a 1:1 molar ratio, adding exactly 0.14 mL of acetic acid. Then, 2 mL of water and 2 mL of hexane were added, mixing the solution vigorously in a vortex and centrifuging at 5000 rpm for 5 min. The hexane phase obtained was transferred to a vial (vial 1) using a Pasteur pipette, whereas an additional 1 mL of hexane was added to the aqueous phase, repeating the stirring and centrifugation process. During this time, anhydrous sodium sulphate was added to vial 1 in order to remove the water, transferring the dehydrated extract to a second vial (vial 2) using a different Pasteur pipette. The additional hexane phase was also added to vial 1, it was dehydrated with anhydrous sodium sulphate and then transferred to vial 2. The hexane in vial 2 was evaporated with a nitrogen current (N_2) until it was reduced to approximately 1 mL. Lastly, the empty vial for chromatography was weighed, the hexane extract was transferred to this vial, it was weighed once again, and the analysis in the chromatograph was conducted.

The lipid profile was determined, following the method described by Abida et al. (2015), through gas chromatography coupled to a Shimadzu mass spectrometry detector (GCMS-TQ8030).

The fatty acids were quantified through the characteristic masses of each of the ions of saturated, monounsaturated and polyunsaturated fatty acids.

The peaks were confirmed using Nist14 MS Database software, which identified each of the fatty acids present in the different samples as a function of the ruptures of the ions and the proportion among the different masses.

The semiquantitative determination of the amount of each of the fatty acids was performed through the sum of the areas of the different acids identified in the species, calculating the percentage of each fatty acid present in the sample.

2.5. Ultrasound-assisted cold alkaline extraction (CAE)

This procedure is applied to the residual solid that remains after extracting the oils of SCG. The result of the extraction is a post-hydrolysis liquid (CAE liquor), from which the hemicelluloses are obtained through a precipitation process, as well as a post-hydrolysis solid, which is chemically and energetically characterised and subsequently subjected to pyrolysis.

The alkaline extraction is performed in a Power Sonic 500 series ultrasound bath, using a constant liquid/solid ratio of 15 Kg of water per Kg of raw material on a dry basis (odb). The independent operational variables of the process were: temperature (40 °C), time (90 min), and sodium hydroxide concentration (100 g L^{-1}), establishing the variables optimised by García et al. (2013).

The resulting CAE liquor was filtered and the solid residue was washed with water. These optimal extraction conditions were established and founded on the need to guarantee the reproducibility of the results and facilitate the comparison with previous studies conducted with other raw materials. By employing the same experimental conditions, the effect of non-controlled variables is minimised, and the reliability of the obtained data is maximised. Moreover, the previous optimisation of these variables ensures that the experiment is carried out within the range of conditions that maximise the yield and quality of the extract, thereby preventing the need for performing numerous preliminary experiments.

Ultrasound-assisted extraction has emerged as a promising technique in the attainment of compounds from plant matrices. Acoustic cavitation, induced by ultrasound, generates microbubbles that collapse, creating extreme conditions of temperature and pressure. These phenomena favour the disruption of cell walls, increasing the contact surface between the solid matrix and the solvent. Furthermore, sonification improves mass transfer, accelerating the dissolution and extraction of the compounds of interest. As a result, greater yields and extraction rate are obtained with respect to conventional methods, without compromising the quality of the extracts (Lozano-Calvo et al., 2024).

Then, the post-hydrolysis solid was air dried to determine the moisture content, and it was weighed to calculate the yield of the process. This solid fraction was chemically characterised, and the energetic parameters were determined, using the same experimental methods that were applied to the raw material.

2.6. Precipitation hemicelluloses in the CAE liquor

Precipitation of hemicelluloses in the CAE liquor is carried out with ethanol after adjusting the pH. To this end, the liquid phase of the extraction was set to pH 4.5–5.5 using 37% HCl. Then, 4 volumes of 95% ethanol were added, and the liquor was centrifuged at 4500 rpm for 3 min. Subsequently, the precipitate was washed with 95% ethanol and was then freeze-dried (García et al., 2013).

2.7. Experimental design for the attainment of furfural through the acid hydrolysis of hemicelluloses

For the acid hydrolysis of the hemicelluloses obtained from the CAE liquor, a central-composition experimental design was developed, which allowed analysing the influence of the independent variables, i.e., temperature (T) and sulphuric acid concentration (X_c), on the dependent variable (furfural estimate), with the aim of optimising one point of the design and maximising the extraction of furfural.

The number of tests required (N) was calculated as: $2^n + 2n + n_C$, where 2^n is the number of points that constitute the design, 2n is the number of axial points and n_C is the number of central points.

The independent variables were normalized following Eq. (1)

$$X_n = \frac{2\cdot(X - \overline{X})}{X_{max} - X_{min}} \quad (1)$$

where:

X: is the absolute value of the independent variable; $\overline{X}$: is the mean value of the variables; and X_{max} and X_{min}: are the maximum and minimum values of the variable, respectively.

The hydrolysis was carried out in a 2-litre Parr reactor. The experiments were designed with two independent variables: acid concentration (X_c) (1, 2 and 3%) and process temperature (X_T) (150, 160 and 170 °C). Time was set at 60 min, with a 1/15 hydromodule. Minimum, mean and maximum values were defined for each of these variables, with a total of 10 experiments.

The methodology used to estimate the furfural content was ultraviolet-visible spectroscopy (UV–vis) (UV Genesus 10 Thermo), equipped with 1 cm optical path length quartz cuvettes.

In the spectroscopic analysis, the calibration curve was created from standard Sigma-Aldrich solutions with a furfural concentration of 1–20 ppm. A sweep was performed for wavelengths of 200–800 nm (results not shown) and a peak was detected in the furfural pattern between 272 and 282 nm. The wavelength used was 277 nm, based on the work of (Heggset et al., 2017). Each experimental value was the mean value of five results. The deviations of the respective means were all below 1%. Other authors used a wavelength of 258 nm to measure the degradation matrix of furfural (Manz and Carter, 2017; Nezamzadeh-Ejhieh and Moeinirad, 2011). However, García et al. (2019) employed a wavelength of 270 nm, which is very similar to the ranges used in our study.

The results were employed to establish polynomials for each dependent variable. The polynomials that include the linear and quadratic terms of the independent variables, and their mutual interactions, were adjusted through multiple regression:

$$Y = a_0 + \sum_{i=1}^{n} b_i X_{ni} + \sum_{i=1}^{n} c_i X_{ni}^2 + \sum_{i=1 j=1}^{n} d_{ij} X_{ni} X_{nj} \ (i < j) \quad (2)$$

Variable Y represents the values of the dependent variables, and the

independent variables X_i represent the temperature (X_T) and the acid concentration (X_c), whereas the coefficients a_0, b_i, c_i and d_{ij} are unknown constant characteristics, and their values are estimated through the experimental data. In the equations, only the statistically significant terms were included; these must reach a significance level value $p < 0.05$ in Student's *t*-test or a confidence interval with over 95% probability. The entire modeling treatment was conducted with Statistica v.1.0 software (StatSoft, Inc., Tulsa, OK, USA).

2.8. Kinetic analysis by Flynn-Wall-Ozawa method

Thermogravimetric experiments applied to each of the thermochemical treatments were carried out in Mettler Toledo thermogravimetry analyzer/DSC1 STARe System. Each thermochemical experiment was divided into three phases: (i) heating the sample from 25 to 105 °C with an inert nitrogen flow of 30 mL min^{-1} acting as a sweep gas at a heating rate of 15 °C min^{-1}; (ii) maintaining the temperature at 105 °C for 5 min under the same flow and atmosphere to ensure complete moisture removal; (iii) heating from 105 to 800 °C at different heating rates (5, 10, 15, and 20 °C min^{-1}), using the same nitrogen atmosphere with a flow of 30 mL min^{-1}. The initial sample mass was approximately 10 mg in all cases, and experiments were carried out in triplicate until the standard deviations of the data were <5%.

The Flynn-Wall-Ozawa (FWO) model has been selected on account of its particular advantages in the field of biomass pyrolysis. These advantages arise from its capacity to manage heterogeneous material and overlapping degradation stages, which are commonplace in lignocellulosic residue such as coffee waste. The method is characterised by its ability to ensure reliability, even in circumstances where the degradation pathway involves parallel or competing reactions. This is achieved by decoupling Ea from the reaction mechanism. For instance, studies on coffee husk and residues (Fermoso and Mašek, 2018; Mukherjee et al., 2021) demonstrated that FWO-derived Ea values align well with experimental thermograms, thus validating its suitability for such systems. This consistency enables direct comparison of kinetic parameters across studies, as demonstrated in the present work, thereby facilitating broader insights into the pyrolytic behaviour of coffee waste under varying thermal conditions.

In this sense, the FWO method is a differential isoconversional kinetic model widely employed to analyze solid-state thermal degradation processes without prior assumption of the reaction mechanism. This model leverages thermogravimetric data obtained at multiple heating rates to determine the activation energy (Ea) as a function of conversion (α), thereby accommodating complex multi-step reactions. The central equation of the FWO model (Eq. (3)) is expressed as:

$$\ln(\beta) = \ln\left[\frac{A\,Ea}{R\,G(\alpha)}\right] - 5.331 - 1.052\left(\frac{Ea}{R\,T}\right) \quad (3)$$

In the given context, the symbol β denotes the heating rate (K min^{-1}), the symbol A represents the pre-exponential factor (s^{-1}), R designates the universal gas constant (8.314 J mol^{-1} K^{-1}), T signifies the absolute temperature (K), and G(α) denotes the integral form of the reaction model. The activation energy can be derived from the slope of the linear regression plot of ln(β) against 1/T at constant α. This method enables a model-free evaluation of pyrolysis kinetics, as demonstrated by the regression equation of −1.052Ea/R.

3. Results and discussion

3.1. Chemical characterisation

To evaluate different ways of valorising SCG, it is important to thoroughly analyze its composition. As an agricultural raw material, the composition of this residue may largely depend on a broad variety of factors, such as the type of coffee, the origin of the coffee grains, the growing conditions, the processing methodology, and the preparation method.

For the current work, as was previously mentioned in the Materials and methods section, SCG was collected from several cafeterias of El Carmen campus of the University of Huelva (Spain) (Table 1). The SCG came from roasted coffee, specifically from the commercial brands Saimaza and Bonka. Similarly, to determine the existence of any significant variation in terms of coffee type, SCG from natural coffee for home consumption was also collected. Table 1 includes the calorific value of the different raw materials. After analysing the results, no significant variations were found regarding coffee type or origin.

In regard with the composition of SCG, approximately 50% by weight corresponds to polysaccharides such as cellulose and hemicellulose. The glucan (cellulose) content is very low; in the present work, 10.4% was obtained, which is within the range reported by other authors (8.5–15.5% of the initial raw material).

The content of hemicellulosic compounds is significant. A total of 40.7% was obtained in this study, in line with the value attained by Mata et al. (2018). Xylan content was also considerable, with 38.6%. This hemicellulosic monomer has not been determined or detected by the authors included in Table 1, where mannose is identified as the main sugar monomer of hemicellulose, with percentages ranging between 13.2 and 29.5%.

Lignin reached a content of 23.5%, whereas other authors, such as Battista et al. (2020b), have reported values of 33.5%. The high percentage of lignin grants a high calorific value to SCG, as it presents a calorific value above 20,000 kJ kg^{-1} on its own.

3.2. Energetic characterisation

Table 2 shows the calorific value of SCG for both the initial raw material and the residual solids obtained after extracting the different compounds (oils and hemicelluloses), and it is compared to that of other materials that are commonly used in biomass boilers for energy production.

Furthermore, with a view to a direct energetic exploitation of SCG (in the form of pellets), it is necessary to determine its elemental composition, whose results are also gathered in Table 2, including the results obtained by other authors.

In the current work, a calorific value of 21,560 kJ kg^{-1} was obtained for SCG, which is within the range reported in previous studies (22000–26,000 kJ kg^{-1}). This value is above that of other materials that are commonly employed as fuel, and 11.6% higher than that of eucalyptus wood (Table 2), thus supporting the viability of SCG as an alternative source of renewable and sustainable energy.

The ash content of biomass affects both the manipulation costs and the processing costs of the energy conversion of biomass. The chemical compositions of the ashes are strongly related to operational issues, such as slag, embedding, sintering and corrosion (Cuiping et al., 2004).

The ash content in SCG is 2–3%. Friedl et al. (2005) concluded that the ashes in SCG do not exceed 1.3%, which is below the range of 2–4% of the common solid biomass.

SCG has a greater content in hydrogen (8.7%) than other residual biomasses, such as that of sunflower (5.9%) and mixed briquettes (5.8%).

The nitrogen percentage (1.4–2.11%) (Coelho et al., 2020; Colantoni et al., 2021) is lower than that determined by Stolarski et al. (2019) for mixed briquettes (2.4%).

The sulfur content is higher than that of some plant species such as rice straw (0.29%), wheat straw (0.32%), corn straw (0.21%), and birch (0.20%), and lower than the content of bituminous coal (0.97%). The contents of S and N are lower than those of fossil fuels such as coal, and thus SCG generates fewer polluting gases during its combustion.

In view of these results, it is demonstrated that SCG is an excellent raw material for use as biomass, with excellent calorific value and low ash content, which is in line with the work of other authors such as

Table 1
Chemical composition of coffee grounds with different substances to extract.

Composition	Type of solvent for extraction		
	Ethanol	Hexane	Isopropanol
Extractables (%)	15.3 ± 2.0	9.3 ± 1.5	9.5 ± 2.1
α Cellulose (glucan) (%)	10.4 ± 0.5	10.8 ± 0.7	10.9 ± 0.6
Klason Lignin (%)	23.8 ± 1.4	24.6 ± 1.8	24.4 ± 1.9
Xylan (%)	38.6 ± 1.7	36.2 ± 1.2	36.5 ± 1.4
Araban (%)	2.1 ± 0.3	1.8 ± 0.2	1.6 ± 0.1
Total Hemicelluloses (%)	40.7 ± 2	38.0 ± 1.4	38.1 ± 1.5
HHV, kJ kg^{-1} o.d.b.	21,560 ± 85	21,560 ± 85	21,810 ± 90

Table 2
Higher calorific value (HCV) on a dry basis (o.d.b) and Elemental composition of coffee grounds.

Present study	HCV (J g^{-1} o.d.b)	C (%)	H (%)	S (%)	O (%)	Ashes (%)
Raw material: Spend Coffee Grounds (SCG)	22,787 ± 105	50,8308	7.0463	0.6113	39.0616	2.45
SCG (Ethanol extractables)	21,098 ± 86	51,0506	7.2164	0.1265	39.4565	2.15
SCG (Hexane extractables)	20,959 ± 72	51,0842	6.9828	0.1446	39.7384	2.05
SCG (Isopropanol extractables)	19,583 ± 78	51,1023	7.1256	0.1369	39.5152	2.12
CAE + SCG (Ethanol extractables)*[1]	19,713 ± 54	51.2015	6.5254	0.2452	39.7879	2.24
CAE + SCG (Hexane extractables)*[2]	20,098 ± 93	51.452	6.6412	0.2475	39.2893	2.37
CAE + SCG (Isopropanol extractables)	20,001 ± 66	51.3425	6.5108	0.235	39.5717	2.34

Other materials	HCV (J g^{-1} o.d.b)	C (%)	H (%)	S (%)	O (%)	Ashes (%)
Spend Coffee Grounds (SCG) (1)	21.340–25.860	51.02	7.04	–	39.83	1.8–3.3
Eucaliptus globulus (2)	19.326 ± 84	51.9	6.32	0.01	41.74	0.7–1.2
Wood material (3)	19.578	49.52	6.79	0.03	43.55	1.14
Sunflower stems (4)	17.259 ± 25	50.5	5.9	0.1	34.9	6.9
Olive pruning pellets (5)	18.720 ± 30	46.1	6.4	0	47.2	1.2
Olive pit (6)	18.092 ± 22	49.8	6.1	0.3	43.0	0.8
Sugarcane bagasse (7)	18.687 ± 20	48.5	6.0	0.4	44.1	1.0
Wheat straw (8)	17.493 ± 50	47.9	5.8	0.5	45.0	0.8
Rice straw (9)	15.200 ± 24	46.3	5.6	0.6	46.7	0.8

(1) (Coelho et al., 2020; Colantoni et al., 2021). (2) (Loaiza et al., 2016; Reza et al., 2020). (3) (Friedl et al., 2005). (4) (Caparrós et al., 2008). (5) (Álvarez et al., 2016; García Martín et al., 2011). (6) (Álvarez et al., 2015; Bustamante et al., 2016). (7) (Haro et al., 2024; Silva et al., 1998). (8) (Haro et al., 2024; Nebrahtu et al., 2013). (9) (Haro et al., 2024; Potip and Wongwuttanasatian, 2018)
*[1] Composition of the resulting solid after extraction with ethanol.
*[2] Composition of the resulting solid after ethanol and cold alkaline extractions.

Colantoni et al. (2021), who evaluated coffee briquettes with over 98% in their composition.

3.3. Coffee oil extraction and characterisation

As was previously indicated in the Materials and methods section, different extraction solvents were employed to extract the SCG oils, specifically two polar solvents (ethanol and isopropanol) and a polar solvent (hexane). The yield obtained in oils using these solvents varied between 15.3 and 17.3% for ethanol, 9.3 and 10.8% for hexane, and 9.5 and 11.6% for isopropanol, by dry weight.

Al-Hamamre et al. (2012) obtained similar amounts of oils (15%) employing hexane. These authors attained the best results with hexane as extraction solvent after 30 min, with respect to other solvents, whereas Battista et al. (2020b) obtained 10% of oil from SCG using the same solvent. The variation in results among different authors may be due to the variation in the content of oil as a function of the coffee species, climatic conditions, harvest time, and drying method (Araujo et al., 2022). Moreover, different previous treatments of the raw materials, e.g., boiling, drip brewing or percolation, may lead to different concentrations of substances in SCG (Ahangari and Sargolzaei, 2013).

One of the most popular coffee production methods is the Soxhlet method, since it is easy to apply and does not require high costs or investment, with the most used solvents being ethanol, isopropanol, methanol and, to a greater extent, hexane.

As can be observed in Table 3, the most widely used solvent is hexane, in different extraction methodologies, among which it is worth highlighting the extraction conducted by Sarno and Iuliano (2018) who

Table 3
Chemical composition and energy content of solid residues obtained after alkaline extraction (CAE) of hemicelluloses, following prior oil extraction with different solvents.

Composition ethanol		Composition hexane		Composition isopropanol	
Yield (%)	46.1 ± 4.2	Yield (%)	43.5 ± 2.3	Yield (%)	43.9 ± 1.7
α Cellulose (glucan) (%)	18.3 ± 0.4	α Cellulose (glucan) (%)	21.9 ± 0.6	α Cellulose (glucan) (%)	19.9 ± 0.6
Klason Lignin (%)	41.8 ± 1.3	Klason Lignin (%)	45.2 ± 1.1	Klason Lignin (%)	44.5 ± 1.7
Xylan (%)	13.4 ± 1.3	Xylan (%)	13.7 ± 1.5	Xylan (%)	12.5 ± 1.6
Araban (%)	0.9 ± 0.4	Araban (%)	0.8 ± 0.2	Araban (%)	0.7 ± 0.2
Total Hemicelluloses in solid (%)	14.3 ± 1.7	Total Hemicelluloses in solid (%)	14.5 ± 1.7	Total Hemicelluloses in solid (%)	13.2 ± 1.8
HHV, kJ kg^{-1} o.d.b.	21,529 ± 54	HHV, kJ kg^{-1} o.d.b.	20,098 ± 93	HHV, kJ kg^{-1} o.d.b.	19,583 ± 80

Each value is the average of three samples (Mean ± SD, standard deviation <10%).

obtained up to 19.3% of oils using an accelerated extraction device. Nevertheless, ethanol may present disadvantages.

The solvent that allows for the greatest recovery of oil is octane, although it is also the solvent that takes the longest time to complete the extraction and one of the solvents with the lowest recovery rates. On the other hand, ethanol and hexane have a lower solvent recovery, with the shortest and second longest recovery times, respectively. Hexane is one of the solvents with the greatest recovery. Isopropanol poses a better option in terms of extraction and solvent recovery, followed by a 50:50 (*v*/v) mixture of isopropanol and hexane, which produces a greater oil extraction with a low recovery percentage (Caetano et al., 2012).

Fig. 2 shows the concentration of the main chemicals obtained from SCG using different solvents. The analysed compounds include methyl arachidate (C20:0), methyl linoleate (C18:2), cis C18:1 trans-9 methyl elaidate, methyl stearate (C18:0) and methyl palmitate (C16:0).

The results indicate that methyl palmitate (C16:0) is the compound with the greatest concentration in all extractions, with values close to 40 ppm when hexane was employed. This finding is in agreement with the literature, which reports that palmitic acid is one of the main components of fatty acids in SCG (34%) (Battista et al., 2020a). Similarly, methyl linoleate (C18:2) also presents a considerable concentration, which is in line with its proportion of 37% in the global composition of the extracted fatty acids.

In regard with extraction efficiency, hexane was the most efficient solvent, followed by ethanol and isopropanol. The high efficiency of hexane may be attributed to its apolar nature, which favours the solubilisation of long-chain fatty acids.

On the other hand, methyl arachidate (C20:0) and cis C18:1 trans-9 methyl elaidate were found in lower concentrations in all extractions, which suggests that these compounds have a lower presence in SCG or are less soluble in the solvents used.

The obtained results confirm that SCG contain a significant amount of fatty acids that can be converted to biodiesel through transesterification. Hexane appeared to be the most efficient solvent for the extraction of these compounds, especially in the case of methyl palmitate and methyl linoleate. These findings highlight the potential of using SCG for the production of sustainable biofuels.

3.4. Results of the chemical characterisation after CAE

The solid that remained after extracting the oils was subjected to CAE, with the aim of extracting the hemicelluloses. Table 3 includes the chemical characterisation of the resulting solid obtained with the different solvents.

The solid yield was 5.6% and 4.7% higher using ethanol compared to hexane and isopropanol, respectively.

When hexane was employed, the solid presented a greater percentage of glucan and lignin with respect to the use of the other solvents. The remaining hemicelluloses were similar in terms of xylan (approximately 13.5%) and arabinan (0.7–0.9%).

The calorific value of the solid increased slightly with the use of ethanol, with 21.529 kJ kg^{-1}, which is very similar the calorific value presented by the raw material (21.560 kJ kg^{-1}). This is a positive finding from the perspective of raw material exploitation, since hemicelluloses are obtained and, at the same time, good energetic characteristics are maintained (high calorific value).

The aim is to obtain the maximum amount of hemicelluloses and a remaining post-hydrolysis solid that presents good energetic characteristics.

3.5. Results of the experimental design

An experimental design was carried out with the hydrolysis process on the hemicelluloses extracted in the previous processes, in order to obtain furfural, whose results are shown in Table 4.

As can be observed, Table 4 and Fig. 3 present the estimated results of furfural concentration, with values ranging between 146.6 and 590.3 mg L^{-1}. This variation in concentrations may be attributed to different factors, especially the increase of acid concentration and operating temperature. As these parameters increase, the furfural degradation reactions intensify, which explains the concentration decrease of these compounds in extreme conditions. That is, although the increase of acid concentration and temperature initially favour the formation of furfural, once certain thresholds are exceeded, the equilibrium is displaced toward degradation, which results in a significant reduction of the amount of these compounds.

The most favorable results, in terms of furfural concentration

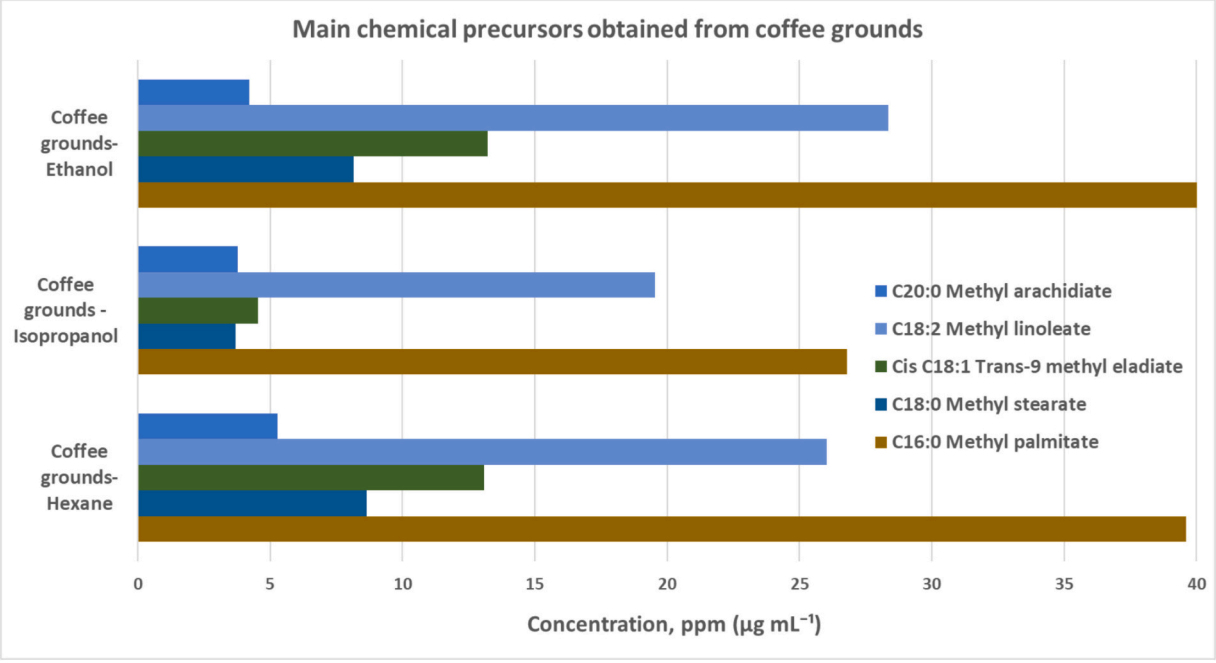

Fig. 2. Main chemical precursors obtained from oils extracted from coffee grounds with different solvents (ethanol, isopropanol and hexane).

Table 4
Furfural yield (mg L^{-1}) obtained from the acid hydrolysis of previously extracted hemicelluloses under different experimental conditions.

N° Exp.	X_a	X_T	Time (min)	Acid (%)	T (°C)	Furfural (mg L^{-1})
1	0	0	60	2	160	590.3
2	0	0	60	2	160	590.3
3	1	1	60	3	170	146.6
4	1	−1	60	3	150	249.3
5	−1	1	60	1	170	264.7
6	−1	−1	60	1	150	367.4
7	1	0	60	3	160	392.5
8	−1	0	60	1	160	510.6
9	0	1	60	2	170	344.4
10	0	−1	60	2	150	447.1

Equation furfural	R^2	F-Snedecor
$F = 590.2 - 59.1\ Xc - 138.4\ XcXc - 194.5\ X_TX_T - 51.4\ X_T$	0.94	45.6

The differences between the experimental values and those estimated by using the previous equation never exceeded 10%.

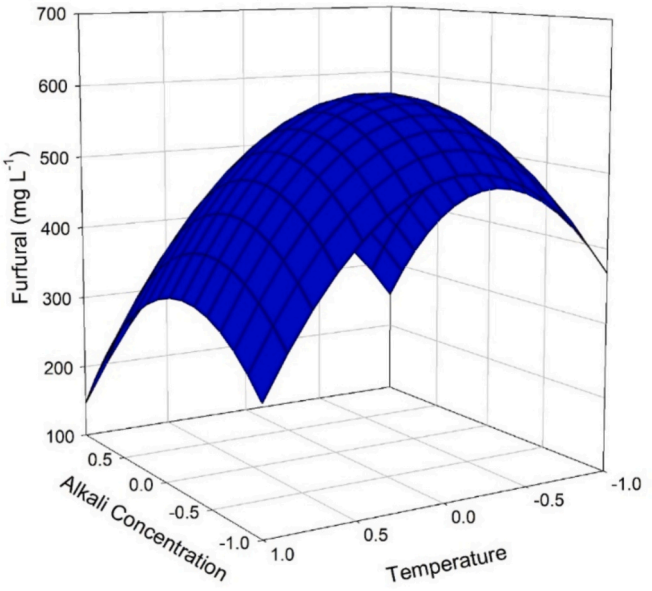

Fig. 3. Furfural variations as a function of temperature and alkali concentration of acid hydrolysis process.

maximisation, occurred in the central conditions of the experiment, where 2% acid and 160 °C were employed. Under these conditions, much higher concentrations were reached, up to 590.3 mg L^{-1}, suggesting that these parameters represent the optimal operating point to maximise the formation of furfural without incurring its accelerated degradation. This tendency is in line with that reported in previous studies, such as that of Heggset et al. (2017), who estimated the concentration of furfural in nanocellulose dispersions after a process of thermal ageing at 140 °C for 3 days, obtaining up to 742 mg L^{-1} of furfural. The similarity of these results suggests that the behaviour of the formation and degradation of furfural under conditions of high temperature is consistent, both in biomass conversion processes and in other lignocellulosic matrices.

The furfural concentrations obtained in this study (146.6–590.3 mg L^{-1}, with an optimum of 590.3 mg L^{-1} at 2% acid and 160 °C) are consistent with trends reported in recent literature for lignocellulosic biomass conversion. Recent studies highlight the potential of hemicellulose-rich residues for furfural production. For example, Pereira et al. (2021, 2019) reported HMF yields from spent coffee grounds ranging between 35 and 47 g kg^{-1} biomass under acidic conditions, while Hu et al. (2023) achieved 11.3 g furfural per 100 g Camellia husks (approximately 113 g kg^{-1}). Similarly, Lima et al. (2024) demonstrated nearly complete xylose conversion to furfural in olive pomace using niobium-based catalysts. Although these values are expressed per unit of biomass rather than per liter, they indicate that furfural production from lignocellulosic residues can reach tens of grams per kilogram, which aligns with our results when normalized to biomass loading (aproximately 180 g kg^{-1} SCG). This comparison reinforces the relevance of our findings and confirms that the optimal conditions identified are competitive with, and in some cases exceed, those reported for other feedstocks. Furthermore, the observed degradation at extreme conditions agrees with previous findings, emphasizing the importance of balancing furfural formation with the minimization of secondary products.

It is important to point out that the aim of selecting the optimal conditions is not only the maximisation of furfural concentration, but also the minimisation of undesirable subproduct formation, which can hinder the separation and purification of these compounds. At higher temperatures and acid concentrations, secondary compounds tend to appear, such as levunilic, formic and acetic acid, which may have a negative effect on the global yield of the process. For instance, studies like that conducted by Zhang et al. (2016) report that the degradation of furfural under conditions of high acidity and temperature is an unavoidable phenomenon if the reaction time is not strictly controlled.

Therefore, selecting an optimal reaction point must not only be focused on the maximum concentration of furfural, but also on balancing the formation of useful intermediate products with the prevention of degradation. In this context, the values observed in Table 4 for the conditions of 4% acid and 160 °C are highly promising, since they are within the upper limit of furfural concentration, while minimising the production of degradative subproducts.

Another relevant aspect is the scalability of these conditions. Although the laboratory experiments proved to be effective in obtaining high yields of furfural under these conditions, their viability at the industrial level depends on the capacity to accurately control the temperature and acidity conditions in large-scale systems. Studies such as that of Edumujeze et al. (2025) suggest that, in industrial-scale processes, heat transfer and pH control may be more difficult to manage, which could result in a greater variation of product concentrations. However, the optimisation of the experimental conditions on a small scale continues to be a crucial step for the design of efficient industrial processes.

It is worth highlighting that the selection of raw materials also plays a critical role in the production of furfural. Lignocellulosic residues, such as agricultural subproducts, are sources rich in pentoses and hexoses, which are the direct precursors of these compounds. Nevertheless, the composition of these residues may vary significantly depending on the source, which can also influence the final concentrations of furfural obtained under optimal conditions. For example, sugarcane bagasse, which contains high levels of hemicellulose, is an excellent source of pentoses, whereas residues of crops such as corn and wheat straw may present greater hexose concentrations, which favours production (Girisuta et al., 2006). Thus, the adaptability of these optimal conditions to different types of biomasses is a key research area that must be explored in future studies, in order to maximise the production potential of these valuable compounds.

It has been demonstrated that furfural is one of the most abundant gas products of the degradation of hemicelluloses, and it may be considered as a convenient product for use in the manufacture of biodiesel (Łojewski et al., 2010).

3.6. Thermogravimetric analysis (TGA) of the pyrolytic process

The thermogravimetric analysis (TGA) Fig. 4, of raw coffee residue and its solvent-extracted derivatives reveals distinct degradation

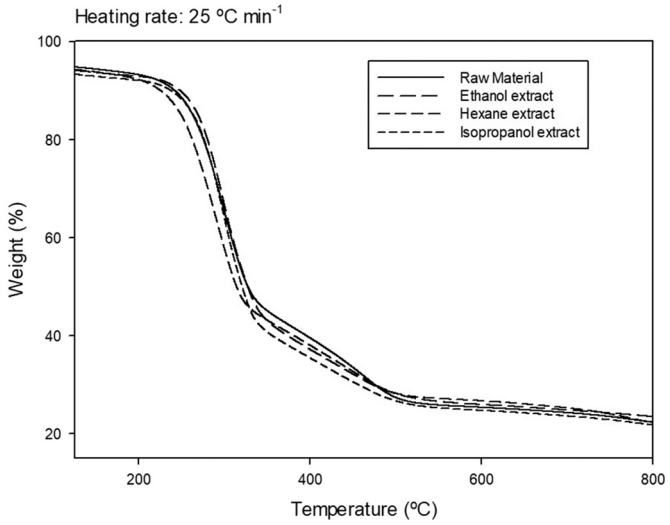

Fig. 4. TGA at different heating rates of the raw material and the four post-CAE solid phases.

patterns, which correlate with their chemical compositions (Table 1). The raw material exhibits a three-stage decomposition: initial moisture loss (30–150 °C), followed by hemicellulose/cellulose degradation (200–350 °C), and lignin/lipid decomposition (350–500 °C). It is noteworthy that the ethanol-extracted sample exhibited a higher extractable content (≃15%) in comparison to hexane (≃10%) and isopropyl alcohol (IPA, ≃10%). This observation is consistent with the ethanol-extracted sample demonstrating elevated volatile removal during the initial stage of the process. This finding lends further credence to the hypothesis that ethanol is an effective extraction agent for polar compounds, such as low-molecular-weight carbohydrates or phenolics, as evidenced by previous studies (Rijo et al., 2021). During the second stage (200–350 °C), as shown in Table 1, the hemicellulose content of the raw material (≃40%) is associated with significant weight loss. However, the process of ethanol extraction leads to a reduction in the levels of xylan and arabin, resulting in a 5–7% decrease in the hemicellulose content of the extracts. This observation is consistent with the ethanol extract exhibiting a marginally reduced weight loss of approximately 38%, in comparison to the raw material, which experienced a loss of around 41%, within this specific range. Hexane and IPA extracts, with lower extractables and similar cellulose/hemicellulose profiles to the raw material, exhibit comparable degradation in the 200–350 °C range. However, the preferential removal of non-polar lipids by hexane (Polat and Sayan, 2023) results in a diminution of weight loss at temperatures of 350–400 °C, where lipid decomposition becomes predominant. The residual lignin content (approx. 24% across all samples) guarantees ongoing char formation above 500 °C, with hexane displaying a marginally higher residual mass (≃25%), presumably due to its reduced lipid interference. These findings are consistent with the observations reported by Mukherjee et al. (2021), who noted that the process of solvent extraction modifies the reactivity of feedstock materials by altering the lignocellulosic composition. It is evident that, in general, the process of ethanol extraction serves to enhance the removal of volatile substances. Conversely, hexane optimises thermal stability for the purpose of char production. This observation is consistent with the conclusions of studies conducted on coffee waste, which have demonstrated that hexane-soluble fractions are characterised by a high lipid content (Go et al., 2020). The isopropyl alcohol extract demonstrates intermediate behaviour, exhibiting moderate weight loss across all stages. This phenomenon is potentially attributable to its limited polarity, which extracts a lower number of polar compounds in comparison to ethanol. The residual mass at elevated temperatures (>500 °C) is observed to be greatest in the hexane extract, suggesting the presence of higher ash content or thermally stable compounds remaining after lipid removal. In comparison, the raw material exhibits the most intricate composition, while solvent extracts selectively reduce particular components, thereby altering thermal stability.

3.7. Derivative thermogravimetry (DTG)

On the other hand, the derivative thermogravimetric (DTG) Fig. 5, curves have been shown to highlight the degradation kinetics of coffee waste components. The raw material displays two prominent peaks: a sharp peak at approximately 300 °C (corresponding to cellulose decomposition) and a broader peak at approximately 380 °C (corresponding to lignin/lipid degradation). The ethanol-extracted sample displays diminished peak intensity at 300 °C (derivative weight loss: 12.5 mg min^{-1} compared to 14.2 mg min^{-1} in the raw material), which is ascribed to its reduced hemicellulose content (≃38%). This data is consistent with the observations reported by Tibola et al. (2020), who noted that the removal of hemicellulose leads to a decrease in the rate of cellulose decomposition, a phenomenon attributable to the reduction in catalytic interactions between the constituent components. Moreover, the DTG profile of the hexane-treated sample shows a reduced peak at 380 °C (8.7 mg min^{-1} derivative weight loss vs. 10.1 mg min^{-1} for the raw material), consistent with lipid extraction (≈9% extractives). Lipids, which undergo exothermic decomposition at elevated temperatures (Fermoso and Mašek, 2018), have been shown to contribute to rapid mass loss; their removal has thus been demonstrated to slow degradation kinetics in this region. In contrast, the process of IPA extraction exerts a minimal effect on DTG profile, resulting in the presence of a residual shoulder near 320 °C. This observation is indicative of the retention of semi-polar compounds, such as waxes, which have been shown to influence the mechanisms of lignin degradation.

The higher peak magnitudes of the raw material demonstrate its inherent reactivity, which leads to rapid devolatilisation. However, hexane's reduced lipid content has been demonstrated to lower energy release with the potential to improve bio-oil stability by minimising secondary cracking (Abdallah et al., 2023). These kinetic insights emphasise that solvent extraction modifies the decomposition mechanisms, enabling targeted valorisation, hexane for stable bio-oil, ethanol for syngas, and raw residue for balanced outputs. In this regard, the analysis of DTG data has revealed that extraction exerts a substantial influence on the rates and mechanisms of degradation. This alteration is contingent upon the polarity and selectivity of the solvent. The suppression of hemicellulose-driven peaks by ethanol indicates a shift toward lignin-dominated degradation, which has the potential to enhance

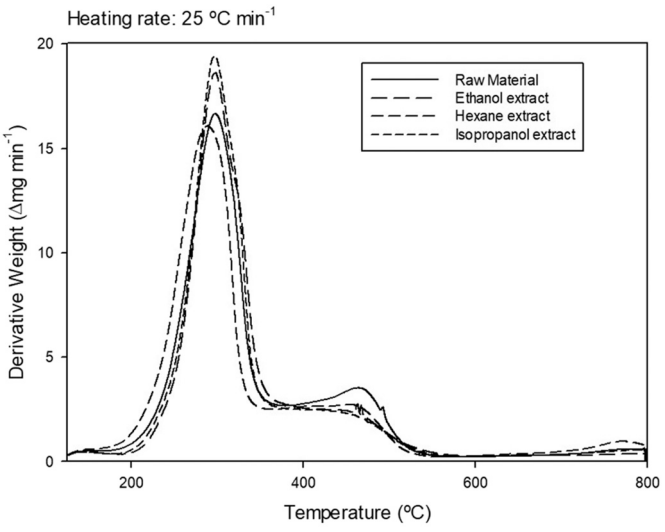

Fig. 5. DTG of the raw material and the four post-CAE solid phases.

syngas quality due to increased H_2 yields from lignin aromatics (Rijo et al., 2021). These kinetic insights emphasise that solvent extraction modifies decomposition mechanisms, thereby enabling targeted valorisation, hexane for stable bio-oil, ethanol for syngas, and raw residue for balanced outputs. In this regard, the analysis of DTG data indicates that extraction exerts a substantial influence on the rates and mechanisms of degradation. This alteration is contingent upon the polarity and selectivity of the solvent.

3.8. Kinetic analysis of the pyrolytic process

As can be seen in Fig. 6, the evolution of activation energy (Ea) as a function of conversion (α = 0.3–0.6) for raw coffee residue and its solvent-extracted derivatives (ethanol, hexane, and isopropyl alcohol) is illustrated by using the FWO method. The raw material displays a significant increase in Ea (100–400 kJ mol^{-1}) with conversion, indicating a shift in pyrolytic mechanisms as degradation progresses. This observation is congruent with the intrinsic complexity of biomass decomposition, wherein the initial stages (low α) encompass volatile and hemicellulose-rich components requiring lower energy, while the elevated conversion stages (α > 0.5) involve recalcitrant lignin, demanding elevated Ea. In comparison, solvent-extracted residues manifest distinct Ea profiles. The ethanol extract demonstrates a moderate Ea range (150–350 kJ mol^{-1}), which is presumably attributable to the elimination of polar compounds (e.g., phenols, carbohydrates). This process results in the retention of a cellulose-enriched matrix that exhibits intermediate stability. In contrast, the hexane extract exhibits higher Ea values (200–400 kJ mol^{-1}), attributable to the selective extraction of non-polar lipids, which concentrates lignin biopolymer with inherently high thermal resistance, as noted by (Fermoso and Mašek, 2018), who reported lignin Ea ≈ 266 kJ mol^{-1}. The isopropyl alcohol extract demonstrates intermediate behaviour, possibly due to its ability to solubilise both polar and semi-polar compounds, creating a mixed biopolymer matrix. These results are consistent with the data reported by Mukherjee et al. (2021), who observed Ea ranges of 62–140 kJ mol^{-1} for exhausted coffee residues (ECR) using FWO. The current study observes significantly higher Ea values, which may be attributed to differences in feedstock composition or extraction protocols, which alter the relative proportions of cellulose, hemicellulose, and lignin. It is noteworthy that the divergence in Ea at higher conversion (α > 0.5) underscores lignin's dominance in later pyrolysis stages, which is consistent with the observations reported by Fermoso and Mašek (2018) on the slow decomposition of lignin. Furthermore, Santos et al. (2020) emphasised that defective coffee beans manifest variable Ea due to compositional heterogeneity, thereby further substantiating the impact of pre-treatment on kinetic parameters. In this sense, it can be posited that ethanol-extracted residues, with a lower Ea, may favour faster degradation at moderate temperatures. Conversely, hexane-extracted residues require higher energy inputs, aligning with reactor designs that prioritise lignin valorisation.

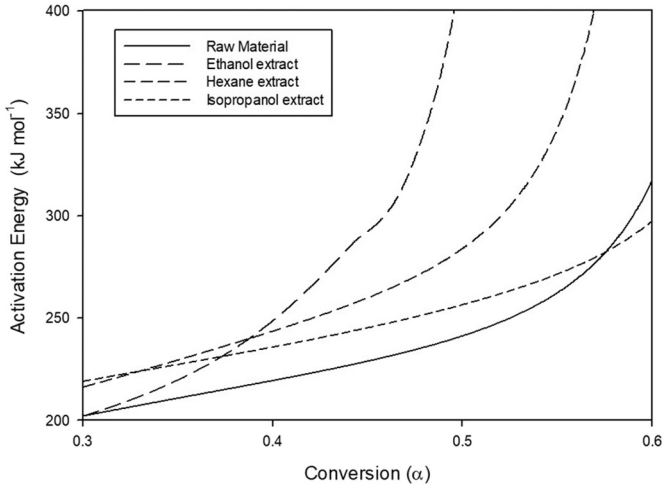

Fig. 6. Activation energy change with post-CAE solid phases.

3.9. Overall mass balance of products obtained in a biorefinery process

The comprehensive valorization strategy for spent coffee grounds (SCG) is founded upon a cascading biorefinery approach, the material flow of which is schematically represented in Fig. 1 (Section 2.1). To establish a precise mass balance and accurately quantify process yields, a functional starting unit of 1000 g (1 kg) of SCG was defined. It is important to note that all calculated balances and yields have been estimated based on the specific methodologies employed for each process stage, ensuring that experimental data deviations do not exceed 10%.

The process commences with a solid-liquid extraction aimed at recovering the lipid fraction. Although the study comparatively evaluated the use of hexane and isopropanol (data presented in Table 1), ethanol was selected as the optimal solvent, justified by both its extractive efficiency and its environmental sustainability profile, which facilitates its subsequent recovery via distillation. This initial stage yielded a mass recovery of 173 g kg^{-1} SCG, corresponding to an extraction yield of 17.3%. The extracted lipid fraction was then subjected to transesterification, resulting in 82.0 g kg^{-1} SCG of high-value chemical precursors (principally methyl palmitate C16:0, methyl linoleate C18:2, methyl elaidate C18:1, methyl stearate C18:0, and methyl arachidate C20:0). This step confirmed the viability of obtaining key biodiesel precursors with a conversion yield of 48.0% relative to the extractables.

The solid residue remaining after the lipid extraction was subsequently subjected to a cold alkaline extraction (CAE), effectively fractionating the biomass into two streams. 391 g kg^{-1} SCG of solid residue, rich in cellulose and lignin, were recovered (a yield of 46.1%). A portion of this solid was thermally valorized via pyrolysis, producing Biochar with a mass of 140.7 g kg^{-1} SCG, which corresponds to a yield of 36%. Concurrently, the post-alkaline extraction liquid phase showed a high content of soluble hemicelluloses, quantified at 436 g kg^{-1} SCG (a yield of 53.9%).

Finally, the hemicelluloses present in the liquor were recovered through precipitation, obtaining 305.2 g kg^{-1} SCG of solid (a yield of 73%). This high yield is attributable to the selective nature of the cold alkaline extraction treatment, which helps prevent the degradation of hemicelluloses, thus facilitating the precipitation of the intact fraction. The remaining hemicellulose fraction in the liquid (approximately 27%) is suitable for other applications, such as an additive to cellulose pulp for paper manufacturing. The precipitated hemicelluloses were subjected to an acid hydrolysis process for conversion into furfural. This conversion achieved a yield of 59%, resulting in a final mass of 180 g of furfural per kg of starting SCG. The remaining 41% that does not transform into furfural is not entirely lost but rather subsists in the reaction medium as various byproducts. These include primary intermediates like xylose, as well as other degradation derivatives such as levulinic acid and formic acid.

4. Conclusions

Spent coffee grounds (SCG) represent a promising renewable feedstock for the production of biofuels and value-added chemicals within a circular economy framework. This study demonstrated the feasibility of a multi-stage biorefinery approach, including oil extraction for biodiesel production, hemicellulose recovery via ultrasound-assisted cold alkaline extraction, and furfural synthesis through acid hydrolysis. The process preserved the calorific value of the solid residue, which was further valorized through pyrolysis to obtain biochar. Solvent selection

influenced pyrolysis outcomes: hexane enhanced bio-oil and biochar quality, while ethanol favored syngas and chemical production. Kinetic analysis supported the optimization of hydrolysis conditions for furfural yield. Overall, SCG valorization through integrated thermochemical and biochemical processes offers a sustainable pathway for waste reduction and renewable energy generation. These findings support the development of flexible, low-impact biorefineries tailored to specific product streams and industrial applications.

CRediT authorship contribution statement

Javier Mauricio Loaiza: Methodology, Investigation, Data curation, Conceptualization. **Alberto Palma:** Validation, Methodology, Formal analysis. **Juan Carlos Garcia:** Software, Resources, Funding acquisition. **Manuel Jesús Diaz:** Writing – review & editing, Visualization, Supervision. **Ascensión Alfaro:** Writing – review & editing, Validation.

Declaration of competing interest

The authors declare that they have no known competing financial interests or personal relationships that could have appeared to influence the work reported in this paper.

Acknowledgements

The authors want to acknowledge the financial support from EPIT-Feder 2021–2027, University of Huelva, "Cascade biorefinery from agroforestry waste and energy crops within the framework of the circular economy" (EPIT1382023). And Spanish Ministry of Science, Innovation and Universities, Grant proyect: "Forest waste and high productivity hardwoods species hydrolytic and thermochemical biorefinery for obtaining value-added chemicals", (REF: MICIIN PID2020-112875RB-C21), and Dr. Javier Mauricio Loaiza thanks a the co-funded by Junta of Andalusia (Spain) through post-doctoral Grant No. DC 21_00664.

Data availability

No data was used for the research described in the article.

References

Abdallah, B.A., Ben Hassen Trabelsi, A., Navarro, M.V., Veses, A., García, T., Mihoubi, D., 2023. Pyrolysis of tea and coffee wastes: effect of physicochemical properties on kinetic and thermodynamic characteristics. J. Therm. Anal. Calorim. 148, 2501–2515. https://doi.org/10.1007/s10973-022-11878-4.

Abida, H., Dolch, L.-J., Meï, C., Villanova, V., Conte, M., Block, M.A., Finazzi, G., Bastien, O., Trichine, L., Bowler, C., Rébeillé, F., Petroutsos, D., Jouhet, J., Maréchal, E., 2015. Membrane glycerolipid remodeling triggered by nitrogen and phosphorus starvation in Phaeodactylum tricornutum. Plant Physiol. 167, 118–136. https://doi.org/10.1104/pp.114.252395.

Acevedo, F., Rubilar, M., Scheuermann, E., Cancino, B., Uquiche, E., Garcés, M., Inostroza, K., Shene, C., 2013. Spent coffee grounds as a renewable source of bioactive compounds. J. Biobaased Mater. Bioenergy 7, 420–428. https://doi.org/10.1166/jbmb.2013.1369.

Ahangari, B., Sargolzaei, J., 2013. Extraction of lipids from spent coffee grounds using organic solvents and supercritical carbon dioxide. J. Food Process. Preserv. 37, 1014–1021. https://doi.org/10.1111/j.1745-4549.2012.00757.x.

Al-Hamamre, Z., Foerster, S., Hartmann, F., Kröger, M., Kaltschmitt, M., 2012. Oil extracted from spent coffee grounds as a renewable source for fatty acid methyl ester manufacturing. Fuel 96, 70–76. https://doi.org/10.1016/j.fuel.2012.01.023.

Ali, F., Saikia, C.N., 1997. Evaluation of Hibiscus sabdariffa and Gamelia arborea as raw materials for production of high a cellulose pulp. JSciIndRes 56, 618–626.

Álvarez, A., Pizarro, C., García, R., Bueno, J.L., 2015. Spanish biofuels heating value estimation based on structural analysis. Ind. Crops Prod. 77, 983–991. https://doi.org/10.1016/j.indcrop.2015.09.078.

Álvarez, A., Pizarro, C., García, R., Bueno, J.L., Lavín, A.G., 2016. Determination of kinetic parameters for biomass combustion. Bioresour. Technol. 216, 36–43. https://doi.org/10.1016/j.biortech.2016.05.039.

Amenaghawon, A.N., Anyalewechi, C.L., Okieimen, C.O., Kusuma, H.S., 2021. Biomass pyrolysis technologies for value-added products: a state-of-the-art review. Environ. Dev. Sustain. 23, 14324–14378. https://doi.org/10.1007/s10668-021-01276-5.

Anagnostopoulou, E., Tsouko, E., Maina, S., Myrtsi, E.D., Haroutounian, S., Papanikolaou, S., Koutinas, A., 2024. Unlocking the potential of spent coffee grounds via a comprehensive biorefinery approach: production of microbial oil and carotenoids under fed-batch fermentation. Environ. Sci. Pollut. Res. 31, 35483–35497. https://doi.org/10.1007/s11356-024-33609-y.

Araujo, M.N., dos Santos, K.C., do Carmo Diniz, N., de Carvalho, J.C., Corazza, M.L., 2022. A biorefinery approach for spent coffee grounds valorization using pressurized fluid extraction to produce oil and bioproducts: a systematic review. Bioresour. Technol. Rep. 18, 101013. https://doi.org/10.1016/j.biteb.2022.101013.

Arora, A., Singh, V., 2020. Biodiesel production from engineered sugarcane lipids under uncertain feedstock compositions: process design and techno-economic analysis. Appl. Energy 280, 115933. https://doi.org/10.1016/j.apenergy.2020.115933.

Ashokkumar, M., 2011. The characterization of acoustic cavitation bubbles – an overview. Ultrason. Sonochem. 18, 864–872. https://doi.org/10.1016/j.ultsonch.2010.11.016.

Atabani, A.E., Al-Rubaye, O.K., 2022. Valorization of spent coffee grounds for biodiesel production: blending with higher alcohols, FT-IR, TGA, DSC, and NMR characterizations. Biomass Convers. Biorefin. 12, 577–596. https://doi.org/10.1007/s13399-020-00866-z.

Barrera-Arellano, D., Badan-Ribeiro, A.P., Serna-Saldivar, S.O., 2019. Corn oil: composition, processing, and utilization. In: Corn. Elsevier, pp. 593–613. https://doi.org/10.1016/B978-0-12-811971-6.00021-8.

Bartolucci, L., Cordiner, S., Di Carlo, A., Gallifuoco, A., Mele, P., Mulone, V., 2024. Platform chemicals recovery from spent coffee grounds aqueous-phase pyrolysis oil. Renew. Energy 220, 119630. https://doi.org/10.1016/j.renene.2023.119630.

Battista, F., Barampouti, E.M., Mai, S., Bolzonella, D., Malamis, D., Moustakas, K., Loizidou, M., 2020a. Added-value molecules recovery and biofuels production from spent coffee grounds. Renew. Sustain. Energy Rev. 131, 110007. https://doi.org/10.1016/j.rser.2020.110007.

Battista, F., Zanzoni, S., Strazzera, G., Andreolli, M., Bolzonella, D., 2020b. The cascade biorefinery approach for the valorization of the spent coffee grounds. Renew. Energy 157, 1203–1211. https://doi.org/10.1016/j.renene.2020.05.113.

Bridgwater, A.V., 2012. Review of fast pyrolysis of biomass and product upgrading. Biomass Bioenergy 38, 68–94. https://doi.org/10.1016/j.biombioe.2011.01.048.

Bustamante, V., Carrillo, A., Prieto, J.A., Corral-Rivas, J.J., Hernández, J.C., 2016. Química de la biomasa vegetal y su efecto en el rendimiento durante la torrefacción: revisión. Rev. Mex. Ciencias For. 7, 5–23.

Butler, E., Devlin, G., Meier, D., McDonnell, K., 2011. A review of recent laboratory research and commercial developments in fast pyrolysis and upgrading. Renew. Sustain. Energy Rev. 15, 4171–4186. https://doi.org/10.1016/j.rser.2011.07.035.

Caetano, Nidia S., Silva, Vania F.M., Mata, Teresa M., 2012. Valorization of coffe grounds for biodiesel production. Chem. Eng. Trans. 26. https://doi.org/10.3303/CET1226045.

Caparrós, S., Ariza, J., López, F., Nacimiento, J.A., Garrote, G., Jiménez, L., 2008. Hydrothermal treatment and ethanol pulping of sunflower stalks. Bioresour. Technol. 99, 1368–1372. https://doi.org/10.1016/j.biortech.2007.01.046.

Carvalho, D.M. de, Queiroz, J.H. de, Colodette, J.L., 2016. Assessment of alkaline pretreatment for the production of bioethanol from eucalyptus, sugarcane bagasse and sugarcane straw. Ind. Crops Prod. 94, 932–941. https://doi.org/10.1016/j.indcrop.2016.09.069.

CEN/TS14918, 2005. Method for the Determination of Calorific Value.

Cheng, H., Zhan, H., Fu, S., Lucia, L.A., 2011. Alkali extraction of hemicellulose from depithed corn stover and effects on soda-AQ pulping. BioResources 6, 196–206. https://doi.org/10.15376/biores.6.1.196-206.

Coelho, J.P., Filipe, R.M., Paula Robalo, M., Boyadzhieva, S., Cholakov, G.St., Stateva, R. P., 2020. Supercritical CO2 extraction of spent coffee grounds. Influence of co-solvents and characterization of the extracts. J. Supercrit. Fluids 161, 104825. https://doi.org/10.1016/j.supflu.2020.104825.

Colantoni, A., Paris, E., Bianchini, L., Ferri, S., Marcantonio, V., Carnevale, M., Palma, A., Civitarese, V., Gallucci, F., 2021. Spent coffee ground characterization, pelletization test and emissions assessment in the combustion process. Sci. Rep. 11, 5119. https://doi.org/10.1038/s41598-021-84772-y.

Couto, R.M., Fernandes, J., da Silva, M.D.R.G., Simões, P.C., 2009. Supercritical fluid extraction of lipids from spent coffee grounds. J. Supercrit. Fluids 51, 159–166. https://doi.org/10.1016/j.supflu.2009.09.009.

Cuiping, L., Chuangzhi, W., Yanyongjie, Haitao H., 2004. Chemical elemental characteristics of biomass fuels in China. Biomass Bioenergy 27, 119–130. https://doi.org/10.1016/j.biombioe.2004.01.002.

de Melo, M.M.R., Barbosa, H.M.A., Passos, C.P., Silva, C.M., 2014. Supercritical fluid extraction of spent coffee grounds: Measurement of extraction curves, oil characterization and economic analysis. J. Supercrit. Fluids 86, 150–159. https://doi.org/10.1016/j.supflu.2013.12.016.

Dhyani, V., Bhaskar, T., 2018. A comprehensive review on the pyrolysis of lignocellulosic biomass. Renew. Energy 129, 695–716. https://doi.org/10.1016/j.renene.2017.04.035.

Edumujeze, D., Fournier-Salaün, M., Leveneur, S., 2025. Production of furfural: From kinetics to process assessment. Fuel 381, 133423. https://doi.org/10.1016/j.fuel.2024.133423.

Efthymiopoulos, I., Hellier, P., Ladommatos, N., Russo-Profili, A., Eveleigh, A., Aliev, A., Kay, K., Mills-Lamptey, B., 2018. Influence of solvent selection and extraction temperature on yield and composition of lipids extracted from spent coffee grounds. Ind. Crop. Prod. 119, 49–56. https://doi.org/10.1016/j.indcrop.2018.04.008.

Efthymiopoulos, I., Hellier, P., Ladommatos, N., Kay, A., Mills-Lamptey, B., 2019. Effect of solvent extraction parameters on the recovery of oil from spent coffee grounds for biofuel production. Waste Biomass Valoriz. 10, 253–264. https://doi.org/10.1007/s12649-017-0061-4.

Fermoso, J., Mašek, O., 2018. Thermochemical decomposition of coffee ground residues by TG-MS: a kinetic study. J. Anal. Appl. Pyrolysis 130, 358–367. https://doi.org/10.1016/j.jaap.2017.12.007.

Forcina, A., Petrillo, A., Travaglioni, M., di Chiara, S., De Felice, F., 2023. A comparative life cycle assessment of different spent coffee ground reuse strategies and a sensitivity analysis for verifying the environmental convenience based on the location of sites. J. Clean. Prod. 385, 135727. https://doi.org/10.1016/j.jclepro.2022.135727.

Friedl, A., Padouvas, E., Rotter, H., Varmuza, K., 2005. Prediction of heating values of biomass fuel from elemental composition. Anal. Chim. Acta 544, 191–198. https://doi.org/10.1016/j.aca.2005.01.041.

García Martín, J.F., Sánchez, S., Bravo, V., Cuevas, M., Rigal, L., Gaset, A., 2011. Xylitol production from olive-pruning debris by sulphuric acid hydrolysis and fermentation with Candida tropicalis. Holzforschung 65, 59–65. https://doi.org/10.1515/hf.2010.113.

García, A., Alriols, M.G., Llano-Ponte, R., Labidi, J., 2011. Ultrasound-assisted fractionation of the lignocellulosic material. Bioresour. Technol. 102, 6326–6330. https://doi.org/10.1016/j.biortech.2011.02.045.

García, J.C., Díaz, M.J., Garcia, M.T., Feria, M.J., Gómez, D.M., López, F., 2013. Search for optimum conditions of wheat straw hemicelluloses cold alkaline extraction process. Biochem. Eng. J. 71, 127–133. https://doi.org/10.1016/j.bej.2012.12.008.

García, M.T., Zamudio, M.A.M., Loaiza, J.M., Morales, A.B., Alfaro, A., Lopez, F., García, J.C., 2019. Characterization and use of southern cattail for biorefining-based production of furfural. Biomass Convers. Biorefin. 9, 333–339. https://doi.org/10.1007/s13399-018-0355-1.

Girisuta, B., Janssen, L.P.B.M., Heeres, H.J., 2006. A kinetic study on the decomposition of 5-hydroxymethylfurfural into levulinic acid. Green Chemistry 8 (8), 701–709. https://doi.org/10.1039/B518176C.

Go, A.W., Pham, T.Y.N., Ju, Y.-H., Agapay, R.C., Angkawijaya, A.E., Quijote, K.L., 2020. Extraction of lipids from post-hydrolysis spent coffee grounds for biodiesel production with hexane as solvent: kinetic and equilibrium data. Biomass Bioenergy 140, 105704. https://doi.org/10.1016/j.biombioe.2020.105704.

Gogoi, D., Kumar, M., Lakshmi, Y.G., 2023. A comprehensive review on “pyrolysis” for energy recovery. Bioenergy Res. 16, 1417–1437. https://doi.org/10.1007/s12155-023-10568-9.

Goh, B.H.H., Ong, H.C., Chong, C.T., Chen, W.-H., Leong, K.Y., Tan, S.X., Lee, X.J., 2020. Ultrasonic assisted oil extraction and biodiesel synthesis of spent coffee ground. Fuel 261, 116121. https://doi.org/10.1016/j.fuel.2019.116121.

Haro, D., Marquina-Barrios, S., Fuentes-Olivera, A., Quezada, A., Cruz-Monzón, J., Cueva-Almendras, L., Morán-González, C., Ventura-Avalos, Y., Rojas-Fermín, J., Barraza-Jáuregui, G., 2024. Compositional and structural characterization of eleven types of lignocellulosic biomass and its potential application in obtaining nanopolysaccharides and producing polyhydroxyalkanoates. Sci. Agropecu. 15, 513–523. https://doi.org/10.17268/sci.agropecu.2024.038.

Heggset, E.B., Chinga-Carrasco, G., Syverud, K., 2017. Temperature stability of nanocellulose dispersions. Carbohydr. Polym. 157, 114–121. https://doi.org/10.1016/j.carbpol.2016.09.077.

Hu, M., Yu, Y., Li, X., Wang, X., Liu, Y., 2023. Towards furfural and biomass char production from Camellia oleifera husks using dilute hydrochloric acid pretreatment: a comprehensive investigation on adsorption performance. RSC Sustain. 1, 1833–1848. https://doi.org/10.1039/D3SU00181D.

Jeníček, L., Tunklová, B., Malaťák, J., Neškudla, M., Velebil, J., 2022. Use of spent coffee ground as an alternative fuel and possible soil amendment. Materials (Basel) 15, 6722. https://doi.org/10.3390/ma15196722.

Jiménez, L., Pérez, I., De la Torre, M.J., García, J.C., 1999. The effect of processing variables on the soda pulping of olive tree wood. Bioresour. Technol. 69, 95–102. https://doi.org/10.1016/S0960-8524(98)00183-7.

Kan, T., Strezov, V., Evans, T.J., 2016. Lignocellulosic biomass pyrolysis: a review of product properties and effects of pyrolysis parameters. Renew. Sustain. Energy Rev. 57, 1126–1140. https://doi.org/10.1016/j.rser.2015.12.185.

Kanaan, A.F., dos Santos, K.C., Menezes, M.A.H., Hamerski, F., Voll, F.A.P., Corazza, M. L., 2025. Sequential extraction of industrial spent coffee grounds using pressurized fluids as solvents. J. Supercrit. Fluids 218, 106503. https://doi.org/10.1016/j.supflu.2024.106503.

Kansai, N., Chaisuwan, N., Supakata, N., 2018. Carbonized briquettes as a tool for adding value to waste from rain tree (Samanea Saman) and coffee ground/tea waste. Eng. J. 22, 47–63. https://doi.org/10.4186/ej.2018.22.6.47.

Khemthong, P., Yimsukanan, C., Narkkun, T., Srifa, A., Witoon, T., Pongchaiphol, S., Kiatphuengporn, S., Faungnawakij, K., 2021. Advances in catalytic production of value-added biochemicals and biofuels via furfural platform derived lignocellulosic biomass. Biomass Bioenergy 148, 106033. https://doi.org/10.1016/j.biombioe.2021.106033.

Kim, J.S., Lee, Y.Y., Kim, T.H., 2016. A review on alkaline pretreatment technology for bioconversion of lignocellulosic biomass. Bioresour. Technol. 199, 42–48. https://doi.org/10.1016/j.biortech.2015.08.085.

Kondamudi, N., Mohapatra, S.K., Misra, M., 2008. Spent coffee grounds as a versatile source of green energy. J. Agric. Food Chem. 56, 11757–11760. https://doi.org/10.1021/jf802487s.

Kovalcik, A., Obruca, S., Marova, I., 2018. Valorization of spent coffee grounds: a review. Food Bioprod. Process. 110, 104–119. https://doi.org/10.1016/j.fbp.2018.05.002.

Lauberts, M., Mierina, I., Pals, M., Latheef, M.A.A., Shishkin, A., 2022. Spent coffee grounds valorization in biorefinery context to obtain valuable products using different extraction approaches and solvents. Plants 12, 30. https://doi.org/10.3390/plants12010030.

Lichtenthaler, F.W., Peters, S., 2004. Carbohydrates as green raw materials for the chemical industry. C. R. Chim. 7, 65–90. https://doi.org/10.1016/j.crci.2004.02.002.

Lima, S., Ricotta, T., García-López, E.I., Liotta, L.F., Villar-Rodil, S., Li Puma, G., Scargiali, F., 2024. Valorization of olive mill waste fractions and production of furfural and 5-hydroxymethylfurfural by heterogeneous catalysis over Nb2O5, NbOPO4 and TiO2-PO4 catalysts. Chem. Eng. J. 497, 154654. https://doi.org/10.1016/j.cej.2024.154654.

Loaiza, J.M., López, F., García, M.T., Fernández, O., Díaz, M.J., Garcia, J.C., 2016. Selecting the pre-hydroloysis conditions for Eucalyptus wood in a fractional exploitation biorefining scheme. J. Wood Chem. Technol. 36, 211–223. https://doi.org/10.1080/02773813.2015.1112402.

Łojewski, T., Sawoszczuk, T., Łagan, J.M., Zięba, K., Barański, A., Łojewska, J., 2010. Furfural as a marker of cellulose degradation. A quantitative approach. Appl. Phys. A 100, 873–884. https://doi.org/10.1007/s00339-010-5663-7.

López, F., García, M.T., Feria, M.J., García, J.C., de Diego, C.M., Zamudio, M.A.M., Díaz, M.J., 2014. Optimization of furfural production by acid hydrolysis of Eucalyptus globulus in two stages. Chem. Eng. J. 240, 195–201. https://doi.org/10.1016/j.cej.2013.11.073.

Lozano-Calvo, S., Loaiza, J.M., García, J.C., García, M.T., López, F., 2024. Ultrasound-assisted cold alkaline extraction: increasing hemicellulose extraction and energy production from populus wood. Forests 15, 109. https://doi.org/10.3390/f15010109.

Manz, K.E., Carter, K.E., 2017. Investigating the effects of heat activated persulfate on the degradation of furfural, a component of hydraulic fracturing fluid chemical additives. Chem. Eng. J. 327, 1021–1032. https://doi.org/10.1016/j.cej.2017.06.168.

Massaya, J., Prates Pereira, A., Mills-Lamptey, B., Benjamin, J., Chuck, C.J., 2019. Conceptualization of a spent coffee grounds biorefinery: a review of existing valorisation approaches. Food Bioprod. Process. 118, 149–166. https://doi.org/10.1016/j.fbp.2019.08.010.

Mata, T.M., Martins, A.A., Caetano, N.S., 2018. Bio-refinery approach for spent coffee grounds valorization. Bioresour. Technol. 247, 1077–1084. https://doi.org/10.1016/j.biortech.2017.09.106.

Mettler, M.S., Vlachos, D.G., Dauenhauer, P.J., 2012. Top ten fundamental challenges of biomass pyrolysis for biofuels. Energ. Environ. Sci. 5, 7797. https://doi.org/10.1039/c2ee21679e.

Mohan, D., Pittman, C.U., Steele, P.H., 2006. Pyrolysis of wood/biomass for bio-oil: a critical review. Energy Fuels 20, 848–889. https://doi.org/10.1021/ef0502397.

Mukherjee, A., Okolie, J.A., Tyagi, R., Dalai, A.K., Niu, C., 2021. Pyrolysis kinetics and activation thermodynamic parameters of exhausted coffee residue and coffee husk using thermogravimetric analysis. Can. J. Chem. Eng. 99, 1683–1695. https://doi.org/10.1002/cjce.24037.

Nebrahtu, Haile, Asfaw, Araya, Asfaw, N., 2013. Investigation of waste coffee ground as a potential raw material for biodiesel production. Int. J. Renew. Energy Res. 3, 854–860. https://doi.org/10.20508/IJRER.23113.

Negawo, A.T., Teshome, A., Kumar, A., Hanson, J., Jones, C.S., 2017. Opportunities for napier grass (Pennisetum purpureum) improvement using molecular genetics. Agronomy 7, 28. https://doi.org/10.3390/agronomy7020028.

Nezamzadeh-Ejhieh, A., Moeinirad, S., 2011. Heterogeneous photocatalytic degradation of furfural using NiS-clinoptilolite zeolite. Desalination 273, 248–257. https://doi.org/10.1016/j.desal.2010.12.031.

Obruca, S., Benesova, P., Kucera, D., Petrik, S., Marova, I., 2015. Biotechnological conversion of spent coffee grounds into polyhydroxyalkanoates and carotenoids. N. Biotechnol. 32, 569–574. https://doi.org/10.1016/j.nbt.2015.02.008.

Pereira, A.P., Woodman, T.J., Brahmbhatt, P., Chuck, C.J., 2019. The optimized production of 5-(hydroxymethyl)furfural and related products from spent coffee grounds. Appl. Sci. 9, 3369. https://doi.org/10.3390/app9163369.

Pereira, A.P., Woodman, T.J., Chuck, C.J., 2021. An integrated biorefinery to produce 5-(hydroxymethyl)furfural and alternative fuel precursors from macroalgae and spent coffee grounds. Sustain. Energy Fuels 5, 6189–6196. https://doi.org/10.1039/D1SE01142A.

Phan, A.N., Phan, T.M., 2008. Biodiesel production from waste cooking oils. Fuel 87, 3490–3496. https://doi.org/10.1016/j.fuel.2008.07.008.

Polat, S., Sayan, P., 2023. Assessment of the thermal pyrolysis characteristics and kinetic parameters of spent coffee waste: a TGA-MS study. Energy Sources Part A Recov. Util. Environ. Eff. 45, 74–87. https://doi.org/10.1080/15567036.2020.1736693.

Potip, S., Wongwuttanasatian, T., 2018. Combustion characteristics of spent coffee ground mixed with crude glycerol briquette fuel. Combust. Sci. Technol. 190, 2030–2043. https://doi.org/10.1080/00102202.2018.1482888.

Ramalakshmi, K., Rao, L.J.M., Takano-Ishikawa, Y., Goto, M., 2009. Bioactivities of low-grade green coffee and spent coffee in different in vitro model systems. Food Chem. 115, 79–85. https://doi.org/10.1016/j.foodchem.2008.11.063.

Reza, M.S., Islam, S.N., Afroze, S., Abu Bakar, M.S., Sukri, R.S., Rahman, S., Azad, A.K., 2020. Evaluation of the bioenergy potential of invasive Pennisetum purpureum through pyrolysis and thermogravimetric analysis. Energy Ecol. Environ. 5, 118–133. https://doi.org/10.1007/s40974-019-00139-0.

Ribeiro, R.C., Mota, M.F.S., Silva, R.M.V., Silva, D.C., Novaes, F.J.M., da Veiga, V.F., Bizzo, H.R., Teixeira, R.S.S., Rezende, C.M., 2024. Coffee oil extraction methods: a review. Foods 13, 2601. https://doi.org/10.3390/foods13162601.

Rijo, B., Soares Dias, A.P., Ramos, M., de Jesus, N., Puna, J., 2021. Catalyzed pyrolysis of coffee and tea wastes. Energy 235, 121252. https://doi.org/10.1016/j.energy.2021.121252.

Santos, C.M., de Oliveira, L.S., Alves Rocha, E.P., Franca, A.S., 2020. Thermal conversion of defective coffee beans for energy purposes: characterization and kinetic modeling. Renew. Energy 147, 1275–1291. https://doi.org/10.1016/j.renene.2019.09.052.

Sarno, M., Iuliano, M., 2018. Active biocatalyst for biodiesel production from spent coffee ground. Bioresour. Technol. 266, 431–438. https://doi.org/10.1016/j.biortech.2018.06.108.

Silva, M.A., Nebra, S.A., Machado Silva, M.J., Sanchez, C.G., 1998. The use of biomass residues in the Brazilian soluble coffee industry. Biomass Bioenergy 14, 457–467. https://doi.org/10.1016/S0961-9534(97)10034-4.

Somnuk, K., Eawlex, P., Prateepchaikul, G., 2017. Optimization of coffee oil extraction from spent coffee grounds using four solvents and prototype-scale extraction using circulation process. Agric. Nat. Resour. 51, 181–189. https://doi.org/10.1016/j.anres.2017.01.003.

Steinbach, D., Kruse, A., Sauer, J., 2017. Pretreatment technologies of lignocellulosic biomass in water in view of furfural and 5-hydroxymethylfurfural production - a review. Biomass Convers. Biorefinery 7, 247–274. https://doi.org/10.1007/s13399-017-0243-0.

Stolarski, M.J., Rybczyńska, B., Krzyżaniak, M., Lajszner, W., Graban, Ł., Peni, D., Bordiean, A., 2019. Thermophysical properties and elemental composition of agricultural and forest solid biofuels versus fossil fuels. J. Elem. https://doi.org/10.5601/jelem.2019.24.1.1819.

TAPPI T204 cm-07, 2007. Solvent Extractives of Wood and Pulp. TAPPI Press, Atlanta.

TAPPI T249 cm-09, 2009. Carbohydrate Composition of Extractive-Free Wood and Wood Pulp by Gas-liquid Chromatography. TAPPI Press, Atlanta.

TAPPI T264-cm-07, 2007. Preparation of Wood for Chemical Anaysis. TAPPI Press, Atlanta, GA.

Tibola, F., de Oliveira, T., Cerqueira, D., Ataíde, C., Cardoso, C., 2020. Kinetic parameters study for the slow pyrolysis of coffee residues based on the thermogravimetric analysis. Quim. Nova 43. https://doi.org/10.21577/0100-4042.20170511.

UNE 16001 EX, 2005. Solid biofuels. In: Method for the Determination of Calorific Value.

Vuppaladadiyam, A.K., Varsha Vuppaladadiyam, S.S., Sikarwar, V.S., Ahmad, E., Pant, K. K., S, M., Murugavelh, S., Pandey, A., Bhattacharya, S., Sarmah, A., Leu, S.Y., 2023. A critical review on biomass pyrolysis: reaction mechanisms, process modeling and potential challenges. J. Energy Inst. 108, 101236. https://doi.org/10.1016/j.joei.2023.101236.

Wang, G., Dai, Y., Yang, H., Xiong, Q., Wang, K., Zhou, J., Li, Y., Wang, S., 2020. A review of recent advances in biomass pyrolysis. Energy Fuel 34, 15557–15578. https://doi.org/10.1021/acs.energyfuels.0c03107.

Yemis, O., Mazza, G., 2012. Optimization of furfural and 5-hydroxymethylfurfural production from wheat straw by a microwave-assisted process. Bioresour. Technol. 109, 215–223. https://doi.org/10.1016/j.biortech.2011.09.122.

Zeitsch, K.J., 2000. The Chemistry and Technology of Furfural and its Many By-Products, 1st Ed vol. 13. Elsevier Science, Köln, Germany.

Zhang, S., Yan, Y., Li, T., Ren, Z., 2005. Upgrading of liquid fuel from the pyrolysis of biomass. Bioresour. Technol. 96, 545–550. https://doi.org/10.1016/j.biortech.2004.06.015.